Final draft published as:

Standfuß, I., C. Geiß, M. Kühnl, A. Droin, J. Mast, M. Wurm, S. Siedentop, B. Heider, and H. Taubenböck. 2023. In the tension between large-scale analysis and accuracy - Identifying and analysing intra-urban (sub-)centre structures comparing official 3D-building models and TanDEM-X nDSMs. Computers, Environment and Urban Systems 102:101953.

DOI: 10.1016/j.compenvurbsys.2023.101953

In the tension between large-scale analysis and accuracy - Identifying and analysing intra-urban (sub-)centre structures comparing official 3D-building models and TanDEM-X nDSMs

Abstract

Intra-urban polycentricity has often been described by a balanced distribution of jobs/residences outside the traditional core cities in so-called (sub-)centres. Recently, this purely socioeconomic view has changed, so that centres are also increasingly understood as a physical manifestation of spatial development policies. Built-up volumes derived from 3D-building models are therefore frequently used instead of or as complement to employment/population figures when studying intra-urban polycentricity. However, such data are expensive and not available universally and permit only geographically limited investigations to date. To overcome this constraint, we investigate whether globally available and consistent TanDEM-X nDSMs (TDX) provide a valid data base for intra-urban polycentricity research based on built-up volumes. Our study focuses on four urban regions in Germany for which we have obtained official 3D-building models (LoD-1). For each study site, we derive aggregated built-up volumes from the TDX and the LoD-1 data and identify (sub-)centres. We use three centre identification algorithms to account for the diversity of methods and outcomes. We consider the LoD-1 (sub-)centres as reference and the TDX (sub-)centres as the entities to be reviewed. First, we quantify their spatial agreement and compare if polycentricity measures calculated based on both data sets lead to similar results. Second, we explore possible causes for discrepancies between the TDX/LoD-1 (sub-)centres. We find high spatial resemblances between TDX and LoD-1 (sub-)centres. Accordingly, we observe that polycentricity measures display similar trends among the two data sets. Nevertheless, we also show that the agreement between TDX and LoD-1 centres can be affected in uneven terrain, in

sparsely built-up areas, and by the algorithms used to identify (sub-)centres. Overall, our results suggest that TDX nDSMs reflect the distribution of built-up structures in sufficient detail so that local-spatial densifications – here equated with (sub-)centres – can be appropriately studied. We therefore conclude that TDX data offer a great potential for the thematic domain of morphological urban analysis at large scale.

Keywords

TanDEM-X, Sentinel, 3D-building models, LoD-1, urban mass concentrations, polycentricity, urban morphology

1) Introduction

Suburbanization trends have led to a decentralization of jobs and households shifting away from traditional urban cores to the hinterlands (Champion 2001, Glaeser and Kahn 2001, Kim 2007). Whether these developments are manifesting in processes of concentration (Garreau 1991, Giuliano and Small 1991, Kloosterman and Musterd 2001) or dispersion (Gordon and Richardson 1996, Lang and LeFurgy 2003) is still an open debate. Nevertheless, the spatial concentration of workplaces/residents outside the core cities has received particular attention in past research and was often addressed under the term "polycentricity".

Polycentricity is a versatile concept that has taken a multitude of definitions in urban and regional studies. At its theoretical core, it paraphrases the existence of multiple (sub-)centres (further referred to as centres) of balanced importance within a specific territorial scope (Parr 2004, Burger and Meijers 2012). What constitutes a centre, depends on the spatial scale on which polycentricity is studied (Zhang and Derudder 2019). Centre structures can be assessed within an urban region (intra-urban) but also between a system of cities (inter-urban) and even among large urban conglomerations (inter-regional) (Hall and Pain 2006). A centre can therefore take many forms, reaching from a small agglomeration of businesses, or a single administrative urban area up to an entire metropolitan region (Taubenböck et al. 2014, Münter and Volgmann 2020).

Over time, numerous analytical methods have been proposed to determine whether an urban system is polycentric. The entry point of every study is the identification of centres (Hall and Pain 2006, Green 2007). On larger scales (inter-urban and inter-regional), administrative units do often sufficiently capture the entities of interest. These are, however, seldom appropriate for identifying small-scale (intra-urban) agglomerations which have advanced independently from official boundaries (Agarwal et al. 2012, Münter and Volgmann 2020). A variety of algorithms have therefore been introduced to delineate intra-urban centres. They range from simple threshold approaches (Giuliano and Small 1991, Wurm et al. 2014, Taubenböck et al. 2017) to more sophisticated locally weighted regressions (McMillen 2001, Krehl 2016). All algorithms share the intent to identify significant local-spatial densifications, usually of jobs or population, within urban regions (Giuliano and Small 1991).

Once centres are identified, the degree to which an urban system is polycentric, can be examined on two different dimensions: a morphological and/or a functional one. Morphological polycentricity is assessed based on attributes of the centres themselves, like population or employment figures (Burger et al. 2011). Functional polycentricity focusses on functional linkages between centres and is frequently investigated with flow data characterizing functional relations (Green 2007, Münter and Volgmann 2020). Currently, many approaches exist that enable to measure the absolute/relative importance of centres – the degree of polycentricity – in urban systems on the two dimensions. The most common ones comprise rank-size-distributions (Burger and Meijers 2012), standard deviation- (Green 2007) and primacy-based indicators (Burger et al. 2011).

Compared to the plethora of theoretical definitions and analytical methods, the input data required for the detection of (intra-urban) centres and/or measuring the balance of importance among them have received little attention. To date, polycentricity is most frequently assessed based on spatially referenced socioeconomic data such as employment/population figures (Krehl and Siedentop 2018, Münter and Volgmann 2020). When these data originate from official surveys, they are often of limited use due to inconsistent data structures and/or censorship guidelines (Taubenböck et al. 2017, Heider and Siedentop 2020). Research investigating polycentricity in urban systems using survey data is therefore regularly restricted to specific regions and small extents, making comparisons between studies challenging or even impossible.

With many authors criticising the lack of cross-national studies (Krehl 2016, Krehl et al. 2016, Heider and Siedentop 2020, Heider et al. 2022), consistent data with extensive spatial coverage are needed. While high-resolution employment data at the spatial level of census districts are for instance freely obtainable in the United States (Graham et al. 2014), comparable data in other countries are often unavailable or have limited access (see e.g. Heider et al. (2022)). Large-scale research using employment numbers is therefore still rare. As far as population figures are concerned, the data situation is more promising. LandScan data, for instance, provides estimates of global population distributions at the level of spatial grids with 1000 m² resolution (Dobson et al. 2000). Given their high spatial resolution and consistency, these data have already been applied in numerous studies addressing polycentric urban development at large scales (e.g. in China: Liu et al. (2017), Liu and Wang (2016) and Li and Derudder (2020)).

However, urban spatial structure is a multifaceted concept (Parr 2004), and employment/population data only capture the socioeconomic dimension (Krehl 2015, 2016). Polycentricity is a characteristic form of the urban spatial structure, with the latter characterizing the organisation of activities/subjects within urban areas (Krehl et al. 2016, Krehl and Siedentop 2018). In addition to market forces affecting the spatial distribution of residents/jobs (Anas et al. 1998), growth management and spatial planning have shaped the spatial configuration of the built environment (Landis 2006, Siedentop et al. 2016b, 2016a) and thus, the physical dimension of urban spatial structure. Centres are consequently not solely clusters of population/jobs but are also increasingly conceived as the physical product of spatial development policies (Taubenböck et al. 2017). Moreover, concentrations of commercial buildings mirror agglomeration economies (e.g. knowledge exchange among employees through proximity), and have been found to resemble employment clusters (Krehl 2015, Taubenböck et al. 2017). Therefore, several scholars have been addressing polycentricity based on physical properties of the built environment instead of or as complement to employment/population figures.

Krehl (2015), Krehl and Siedentop (2018), Taubenböck et al. (2017) and Wurm et al. (2014) for instance, approached intra-urban polycentricity based on built-up structures. By linking individual building footprints with a normalized Digital Surface Model (nDSM) retrieved from Cartosat-1 data (5m spatial resolution) (see Wurm et al. (2014)), they computed building volumes for selected city regions in Germany. The latter were then successfully applied to identify and analyse local-spatial densifications, understood as the structural-physical manifestation of centres. However, Cartosat-1 data is expensive (Taubenböck et al. 2017) and accurate building footprints are not everywhere available. Investigating intra-urban polycentricity based on built-up volumes has consequently only been feasible at limited geographical extents to date.

Recently, Geiß et al. (2019) introduced a procedure that allows for retrieval of spatially distinguished built-up volumes of entire urban regions using on a combination of TanDEM-X (TDX) and Sentinel-2 imagery. Due to the global availability of the two datasets, this method enables to objectively assess and compare the built-up structures of and between virtually every urban region on the planet. Thus, they offer an unprecedented opportunity for consistent and global studies of intra-urban polycentricity based on built-up structures. However, TDX built-up volumes can only be characterized on the level of individual pixels with 12m spatial resolution and are prone to underestimate building volumes (Geiß et al. 2015, 2019). A loss of detail compared to 3D-building models is thus expected. In view of this disadvantage, it remains to be examined whether small-scale spatial densifications of built-up structures within urban systems can still be adequately mapped with TDX data.

Given the aforementioned considerations, we aim to investigate whether built-up volumes derived from globally available TDX data enable to identify and examine intra-urban centres in similar quality than achievable with high-resolution 3D-building models. The remainder of this paper is organized as follows: In Section 2 we introduce the used data as well as the applied methodology and analysis. In Section 3, we present the empirical results of our study: First, the quantified agreement between centre structures in four exemplary city regions derived from 3D-building models and TDX data, respectively, and second, the identified factors influencing this agreement. In Section 4, we then critically discuss the capabilities and limitations of TDX data for intra-urban polycentricity research. Finally, we highlight the implications of our findings for the thematic domain of morphological urban analysis at large scale and conclude the study.

2) Materials and Methods

2.1) Methodological outline of the study

In this study, we focus on the physical dimension of morphological polycentricity at the intra-urban scale. We extract urban mass concentrations (UMC; summed built-up volumes) at the spatial level of regular grids (spatial resolution: 250, 500 and 1000 m²) from 3D-building models (Level of Detail-1 (LoD-1)) and TDX nDSMs, respectively. By this, we generate comparable input data sources for our investigation. We apply different centre identification algorithms and derive one data set with detected high UMC grid cells (hUMC)/ centres (associations of neighbouring hUMC) per input data source, algorithm, and study site. We consider the LoD-1 hUMC/centres as the reference and the TDX hUMC/centres as the entities to be assessed. Based on this setting, we perform a two-step analysis: First, we investigate the spatial agreement between the TDX and the LoD-1 hUMC (spatial resolution: 250, 500 and 1000 m²) and evaluate if the centres (spatial resolution: 1000 m²) retrieved from the two datasets enable to draw similar conclusions regarding the degree of polycentricity/monocentricity in our study sites. Second, we explore causes for discrepancies between the TDX and the LoD-1 hUMC/centres (spatial resolution: 1000 m²). In particular, we focus on the influence of terrain characteristics, built-up structures and functional principles of the centre identification algorithms. A schematic overview of the methodological outline of our study is given in Figure 1.

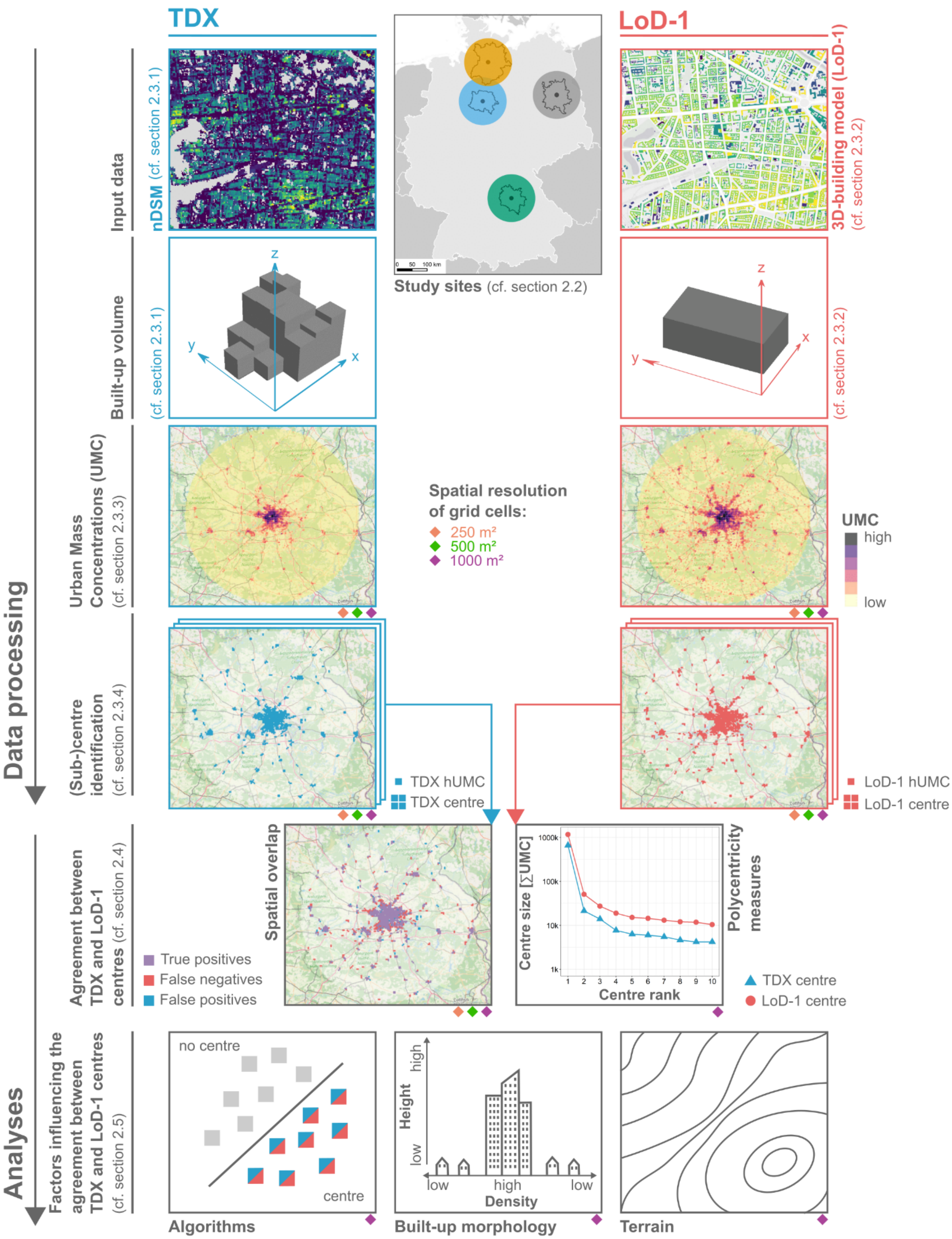

Figure 1: Schematic overview of the methodological outline of this study.

2.2) Study sites

The geographic focus of our study lies on the urban regions of Berlin, Hamburg, Nuremberg and Hanover in Germany (Figure 2: a). We selected these regions because both, LoD-1 (Figure 2: b) and TDX (Figure 2: c) data were available. For each of the considered cities, we determined a location in their city centre using the central points defined in Open Street Map. To generate consistent input data for the centre identification algorithms, we derived equally sized areas with a radius of 80 km around the central locations (Figure 2: a). This scope ensures that our study sites expand only on German territory (see Berlin), while including the administrative area of the core cities as well as large parts of their hinterlands. To compare the degree of polycentricity/monocentricity between the four selected cities, we needed an additional, non-arbitrary delineation of urban boundaries. As suggested in Heider et al. (2022), we used travel time isochrones for this purpose. These encompass the area that can be reached via the road network within a given time starting from the central location. Bearing in mind that larger cities (Berlin, Hamburg) tend to gravitate people from further away than smaller ones (Nuremberg, Hanover), we derived 60- and 45-minute travel time isochrones, respectively (Heider et al. 2022) (Figure 2: a).

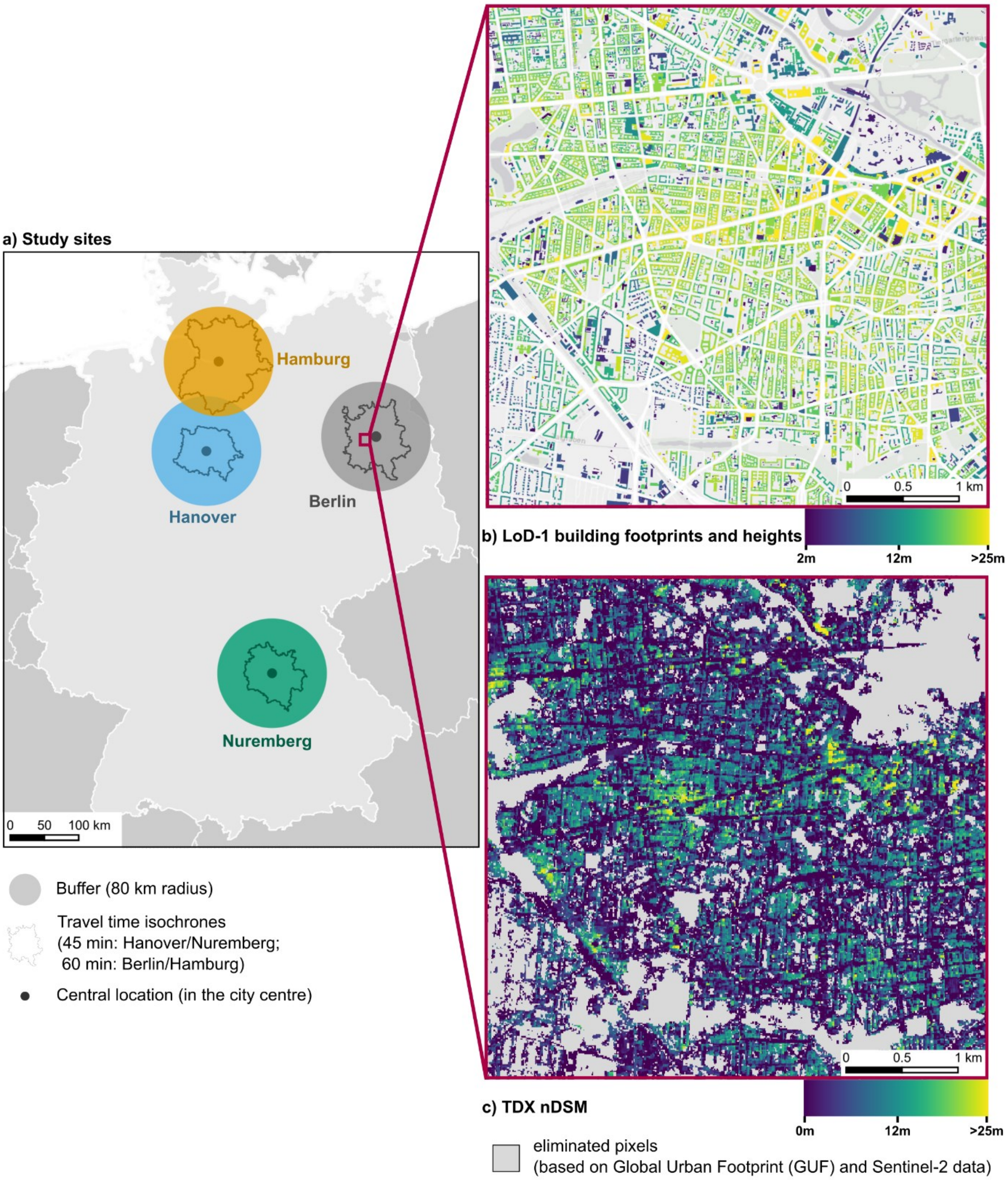

Figure 2: Overview of the study sites (80km buffer/ travel time isochrones around the central locations of Berlin, Hamburg, Hanover and Nuremberg) (a) and the input data sources, LoD-1 building models (b) and TanDEM-X nDSMs (c), of this study.

2.3) Data processing and detection of centres

<u>2.3.1) Derivation of built-up volumes from TDX and Sentinel-2 data</u>

We rely on a combination of a TDX Digital Surface Model (DSM) (recorded 2013-2015; 12m spatial resolution) and Sentinel-2A/B (2015-2017; 10m spatial resolution) data to create the built-up volume datasets to be tested for their suitability in analysing intra-urban polycentricity. To derive the required nDSMs from these data (Figure 1: c), we adhere to the method presented in Geiß et al. (2019): We initially identify "ground pixels" (terrain-only) and "non-ground pixels" (terrain plus objects) in the TDX DSMs. Next, we use the height information of the "ground pixels" to mathematically interpolate a digital terrain model (DTM). By subtracting the DTM from the DSM, we generate a nDSM, which only characterizes the height of objects located on the terrain surface. To eliminate pixels that contain other objects than buildings, we then spatially refine the nDSM by integrating the Global Urban Footprint (GUF) (Esch et al. 2012) and the Sentinel-2A/B data. The GUF aids in limiting the nDSM to predominantly built-up areas while the Sentinel data is used to exclude urban vegetation (Figure 2: c). Finally, we compute built-up volumes for each study site by multiplying the nDSM pixel size with the pixel height.

2.3.2) Derivation of building volumes from 3D-building models

We rely on the official cadastral building model (LoD-1) (BKG 2021) as reference for our study. It provides information on the footprint and height of individual buildings for the entire territory of Germany (Figure 1: b). The building heights of this data set are usually derived from high-resolution (1 m) laser scanning data. Due to the federal administrative structure in Germany, inconsistencies can occur because aggregation methods are not standardized across the country. As a result, some federal states consider the mean and others the median pixel height as reference (ADV 2012). To generate LoD-1 data with equal height reference (median) for our study, we needed to correct the LoD-1 heights of Lower-Saxony (mean). We acquired 166 tiles (1km²) of laser scanning data of the city of Hanover and its surroundings to cover a wide range of building structures. Using these, we derived nDSMs and computed the median heights per building. We then infered several regression equations - one per land use type (residential, commercial, industrial, etc.) - to model the relationship between mean and median building heights. Based on these equations, we calculate median heights for the buildings that are located in Lower-Saxony (Hamburg and Hanover). Lastly, we derive built-up volumes for each study site by multiplying the buildings’ area with their height.

2.3.3) Aggregation of Urban Mass Concentrations (UMC)

To create comparable input data, we migrate the TDX and LoD-1-based built-up volumes to a spatially consistent data structure. We use the European INSPIRE grids in three different resolutions (250, 500 and 1000 m²) as spatial basis (EEA 2017). Grids with 1000 m² resolution are already a standard data basis in several studies addressing intra-urban centre structures (Wurm et al. 2014, Krehl 2015, Taubenböck et al. 2017). We combine the INSPIRE grid with the TDX/LoD-1 data and sum up the built-up volumes of the pixels /buildings located within a grid cell. As a result, we obtain consistent and comparable models of the spatial distribution of urban mass concentrations (UMC) in three different spatial resolutions based on TDX and LoD-1 data for our study sites. In the remainder of this paper, we use the prefixes LoD-1 and TDX to indicate which data set – the LoD-1 building model or the TDX nDSM – is the underlying original data source for the derived UMC and centres (see next section).

2.3.4) Identification of high UMC/ centres

A multitude of methods exists that enable to identify centres, but are known to frequently produce deviating results (Agarwal et al. 2012). To acknowledge this diversity, we apply three centre identification algorithms from two common domains: 1) threshold approaches and 2) locally weighted regression.

First, we use the combined threshold approach published in Taubenböck et al. (2017) (CT-Taubenböck) (1). It applies two thresholds, a regional and a distance-based, in disjunction. The regional threshold was introduced by Wurm et al. (2014). It considers the UMC cells of an entire study site and mainly identifies cells with high UMC (hUMC) belonging to dominant centres (e.g. core cities). Taubenböck et al. (2017) extended this approach by a distance-based threshold. The latter is applied to UMC cells that are grouped into rings based on their distance to the centre (in 1km steps). This approach enables to detect less pronounced local UMC densifications and can identify hUMC cells that are otherwise outshined by dominant centres. With the CT-Taubenböck algorithm, a UMC cell is designated as hUMC when it exceeds the regional and/or distance-based threshold. Both are set to 1.3 times the standard derivation of the respective region/ring. This cut-off value was determined empirically by Taubenböck et al. (2017) to best reflect local centre structures.

Additionally, we identify centres with methods from the locally weighted regression (LWR) family (2). The LWR was initially proposed as a means for centre detection based on spatial employment distributions by McMillen (2001) and comprises a two-step procedure: First, a smoothed surface of the natural logarithm of employment densities of a study site is derived using a LWR approach. Based on the idea that centres are characterized by densities that surpass those of the smoothed surface, spatial units with significant positive residuals are then considered centre candidates. In a second step, multiple semi-parametric regressions are applied iteratively, to remove centre candidates until only those with a significant impact on the overall employment density function remain.

Since its introduction, the LWR was refined several times. Here, we apply two modified LWR versions to identify centres and use UMC instead of employment distributions as input. The first approach was introduced by Krehl (2016) (LWR-Krehl). It differs from McMillen's original method insofar, as it does not use the input data in their logarithmic but in their measured form. Krehl noted, that the former causes a large share of employment densifications to be missed when applied in a German context. As second approach, we use the LWR proposed by Sun (2019) (LWR-Sun). To reduce complexity, Sun applies a simple threshold-based approach instead of iterative regressions to eliminate non-significant centres. For this, we cluster neighbouring hUMC cells (centre candidates) and check if their summed UMC accounts for at least 0.5% (significance threshold) of the total UMC of the study site. By applying the selected procedures, we generate three data sets with identified hUMC cells per input data source (TDX and LoD-1), study site and spatial resolution (250, 500 and 1000 m²).

To determine the centres, we use only the hUMC identified in the grids with 1000 m² spatial resolution, as this is the standard resolution applied in previous research (see 2.3.3). We consider groups of minimum two neighbouring hUMC cells located within the travel time isochrones (see 2.2) henceforth as centres. Therefore, we understand them as clusters of grid cells with significantly higher UMC compared to their surroundings. This physical view of centres stems from earlier studies arguing that commercial hUMC clusters often resemble concentrations of employees and are the physical outcome of the interplay between market forces and spatial development policies (Krehl 2015, Taubenböck et al. 2017).

2.4) Assessment of agreement between TDX and LoD-1 hUMC cells/centres

First, we examine the agreement between the hUMC cells/centres that were identified based on LoD-1- and TDX data, respectively.

Initially, we assess the spatial overlap between the TDX- and the LoD-1-based hUMC cells (spatial resolution: 250, 500 and 1000 m²) (*grid-cell-based agreement*). We treat this investigation as a classification problem in which TDX hUMC represent the result and LoD-1 hUMC the reference. For each study site and centre identification algorithm, we determine the number of true-positive (TP), false-positive (FP), true-negative (TN) and false-negative (FN) hUMC cells. We then derive three accuracy metrics – Recall, Precision and Cohen's Kappa (Congalton 1991) – to measure different aspects of the agreement. Recall quantifies the percentage of LoD-1 hUMC cells (reference) that are correctly identified with TDX hUMC cells. Precision measures the proportion of all identified TDX hUMC cells that are actual LoD-1 hUMC grid cells. These metrics can be computed as follows:

$$Recall = \frac{TP}{TP + FN}$$

$$Precision = \frac{TP}{TP + FP}$$

Cohen’s Kappa quantifies the inter-rater agreement between result (TDX) and reference data (LoD-1). It can be calculated using the following equation:

$$Kappa = \frac{2 * (TP * TN - FN * FP)}{(TP + FP) * (FP + TN) + (TP + FN) * (FN + TN)}$$

Kappa values can range from -1 to 1 and we allocate them to six classes grading the overall “strength of agreement” – from “poor” (Kappa <= 0) to “almost perfect” (Kappa > 0.8) – as proposed in Landis and Koch (1977).

Additionally, we evaluate whether TDX- and LoD-1 centres (spatial resolution: 1000 m²) enable to draw similar conclusions regarding the degree of polycentricity/monocentricity in our study sites (*centre-based agreement*). Morphological polycentricity is typically assessed based on size attributes of centres. Here, we consider the size of a centre by means of its total UMC.

As pointed out by Derudder et al. (2021), there exists a plethora of indicators allowing to evaluate different characteristics of polycentricity. Following the publication from Bartosiewicz and Marcinczak (2020), we compute three polycentricity measures per study site, algorithm and input data source (TDX & LoD-1). These include the Primacy index (Burger et al. 2011), the Rank-size coefficient (Burger and Meijers 2012) and the standard-deviation-based Green index (Green 2007) (Table 1). The Primacy index enables to assess the absolute importance of the largest centre compared to lower-ranked centres and thus, indicates the degree of monocentricity of an urban region. The Rank-size coefficient and the Green index measure the degree of polycentricity more explicitly and are often computed based on a certain number of the largest-ranked centres (Burger and Meijers 2012, Bartosiewicz and Marcinczak 2020). The number of considered centre ranks (N) should be carefully selected to ensure consistency among the indices (Zhang and Derudder 2019). So far, no universally accepted N has been established. We therefore calculate the three indices using different N following a recommendation from Derudder et al. (2021). Specifically, we consider the two up to ten largest-ranked centres (Table 1).

Table 1: Overview of the selected measures used to assess of the degree of (morphological) polycentricity/monocentricity within the study sites.

Index	Source	Equation	Equation parameters	Number (N) of ranked centres	Interpretation	Classification
Primacy index (P)	Burger et al. (2011)	$P = \frac{L_c{}^{max}}{\sum L_C}$	$\boldsymbol{L_c{}^{max}}$: UMC of largest (in terms of totalled UMC) centre of a study site $\sum \boldsymbol{L_C}$: sum of UMC of the considered centre rank	2N (2^{nd}) 3N ($2^{nd}/3^{rd}/4^{th}$) … 10N($2^{nd}/\ldots/10^{th}$)	The lower the value the higher the degree of polycentricity	>0.00 - 0.25 (highly polycentric) >0.25 - 0.50 (polycentric) >0.50 - 0.75 (monocentric) >0.75 - 1.00 (highly monocentric)
Rank-size coefficient (RSC)	Burger and Meijers (2012)	$LN(L_c) = \alpha - \beta LN(R_{c)} + \varepsilon_c$ The RSC then equals the average of β. It is computed multiple times for each group of ranked centres that is considered by a certain N.	$LN(L_c)$: natural logarithm of the UMC within centre c $LN(R_c)$: natural logarithm of the rnak of centre c β: slope of the regression line α: constant ε_c: idiosynchronic error term	2N (2^{nd}) 3N ($2^{nd}/3^{rd}/4^{th}$) … 10N($2^{nd}/\ldots/10^{th}$)	The lower (flatter) the value (slope) the higher the degree of polycentricity	/
Green Index (G)	Green (2007)	$G = 1 - \frac{\sigma_L}{\sigma_{L_{max}}}$ G is computed multiple times for each group of ranked centres that is considered by a certain N	$\boldsymbol{\sigma_L}$: standard deviation of the UMC per centre of the centre group that is considered by N $\boldsymbol{\sigma_{L_{max}}}$: standard deviation of total UMC in a theoretical urban region with two centres. The UMC of the first centre equals zero and that of the second centre equals the UMC of the largest centre in a study site.	2N (2^{nd}) 3N ($2^{nd}/3^{rd}/4^{th}$) … 10N($2^{nd}/\ldots/10^{th}$)	The higher the value the higher the degree of polycentricity	>0.00 - 0.25 (highly monocentric) >0.25 - 0.50 (monocentric) >0.50 - 0.75 (polycentric) >0.75 - 1.00 (highly polycentric)

The values of the Primacy index and the Green index can range between 0 and 1 and a value of 0.5 (Table 1) can be seen as cut-off separating monocentric from polycentric urban systems (Bartosiewicz and Marcinczak 2020). With regard to the Rank-size coefficient, no such clear subdivision is possible, but a lower Rank-size coefficient indicates a higher degree of polycentricity (Burger and Meijers 2012). In view of these schemes, we examine whether the TDX and LoD-1 centres indicate similar polycentricity/monocentricity trends within our study sites.

2.5) Systematic exploration of factors influencing the agreement between TDX and LoD-1 hUMC cells/centres

In the second part of our analysis, we explore causes for discrepancies between the TDX and the LoD-1 hUMC cells/centres (spatial resolution: 1000 m²).

First, we focus on the *functionalities of the centre identification algorithms* (section 2.3.4). TDX built-up volumes underestimate building volumes, particularly at the urban fringes and in the hinterlands (Geiß et al. 2020). Some of the LoD-1 hUMC cells are therefore likely missing from the TDX hUMC cells (FP). Nevertheless, we hypothesize that some of the less pronounced TDX UMC are yet identifiable as hUMC due to the algorithms' specific functionalities. We investigate this exemplarily focussing on one study site: Berlin. We create validation maps displaying the distribution of TP, FP and FN cells per centre identification algorithm. Next, we address the algorithms: The baseline of the LWR approaches is, that the measured UMC distributions are contrasted with smoothed UMC distributions to identify centre candidates. We therefore derive a spatial cross-section of the measured and the smoothed UMC distributions – separately for TDX and LoD-1 - and highlight positive residuals. These distributions show the summed UMC (from East to West) per kilometre from the southern to the northern borders of the study site. We use the measured UMC for the LWR-Krehl approach and the natural logarithm of the measured UMC for the LWR-Sun approach. In the CT-Taubenböck procedure, it is mainly the distance-based approach that enables to spot smaller centres in the suburbs (Taubenböck et al. 2017). We thus obtain a ring-wise spatial cross-section of measured UMC distributions, again considered as totalled UMC (of a ring) per kilometre from South to North. Additionally, we highlight the identified TDX and/or LoD-1 hUMC. By contrasting the UMC distributions with the validation maps, we intend to visually identify agreements/discrepancies between TDX and LoD-1 hUMC that are likely attributable to variations in the algorithms' functionality.

While building heights are generally underestimated by TDX nDSMs, Geiß et al. (2019) identified a mixture of over- and underestimations with regard to built-up densities. They found overestimations primarily in areas with high - and underestimations mainly in regions with low buildings. We therefore assume a relationship between falsely/correctly identified TDX hUMC cells and the *built-up morphology*. For further exploration, we classify the INSPIRE grid cells into nine classes reflecting variations of built-up morphologies in our study sites. This classification is adapted from Geiß et al. (2019) and is based on an ordinal measurement scale representing combinations of low, medium, and high built-up densities (<10, 10-20, >20 %) and heights (<15, 15-25, >25 m). We retrieve the latter information by aggregating the built-up area (sum building area/INSPIRE grid cell area) and height (90th percentile) from the LoD-1 buildings located within an INSPIRE grid cell. We then compute the proportion of TP, FP and FN hUMC cells per morphological class for each study site and centre identification algorithm. By this, we aim to identify matches/mismatches between TDX and LoD-1 hUMC, that are traceable to differences in built-up morphologies.

Terrain characteristics are another factor affecting the quality of TDX nDSMs. Particularly uneven terrain is more challenging to map with TDX DTMs (Geiß et al. 2015). We therefore assume that TDX hUMC cells are prone to mismatch LoD-1 hUMC cells in regions with high relief energy. To explore this further, we characterize the relief energy on the INSPIRE grid level. We incorporate an official DTM with high spatial resolution (25 m), covering the federal territory of Germany (BKG 2016). Using these data, we compute slope values and derive an aggregate for relief energy by calculating the standard deviation (SD) of the slope per INSPIRE grid cell. We suppose higher slope SD values to be indicative for a higher relief energy. By comparing the distributions of the slope SD of TP, FP and FN hUMC cells, we aim to uncover whether certain mismatches between TDX and LoD-1 hUMC are related to terrain characteristics.

3) Results

3.1) Assessment of agreement between TDX and LoD-1 hUMC cells/centres

First, we present the findings of the quantified spatial overlap between TDX and LoD-1 hUMC cells (*cell-based-agreement*) (Figure 3).

1000 m² spatial resolution: Across all study sites, we correctly identify 60 % to 70 % (Recall) of the LoD-1 hUMC with the TDX hUMC using the CT-Taubenböck and the LWR-Sun approach. With Recall values of only 30 % (Hamburg) to 50 % (Berlin), the LWR-Krehl approach identifies a much lower proportion of the LoD hUMC with the TDX hUMC. Of the identified TDX hUMC cells, we observe that 60 % to 90 % (Precision) are also LoD-1 hUMC when considering the CT-Taubenböck and the LWR-Krehl approach. A similarly high Precision can only be achieved in Berlin/Nuremberg with the LWR-Sun approach. In Hamburg and Hanover, Precision values remain below 60 %. In terms of Kappa, the agreement between the TDX and LoD-1 hUMC cells is substantial in all study sites when applying the CT-Taubenböck or the LWR-Sun. However, with the exception of Berlin (substantial), the achievable agreement between the TDX and LoD-1 hUMC is only moderate with the LWR-Krehl.

All spatial resolutions: We observe a decrease in Precision from 1000 to 250 m² spatial resolution among all algorithms (Figure 3: 2). In terms of the Recall, this pattern is repeated only when the CT-Taubenböck is applied. By contrast, no such systematic behaviour is evident with the LWR-Krehl/LWR-Sun, as both, an increase/decrease of the Recall from 1000 to 250 m² resolution can be found among the study sites (Figure 3: 1b/c). However, the Recall values achievable with the LWR-Sun are significantly better than those of the LWR-Krehl. Given these patterns in Precision/Recall, we find the agreement between TDX and LoD-1 hUMC (Kappa) to decrease systematically with increasing spatial resolution with the CT-Taubenböck/LWR-Sun (Figure 3: 3a/c). The agreement between TDX and LoD-1 hUMC from 1000 to 500 m², however, decreases only slightly and thus, remains mostly "substantial" at both spatial resolutions. With the LWR-Krehl by contrast, the pattern of agreement between TDX and LoD-1 hUMC is very heterogenous. In Berlin, for example, the Kappa improves from 1000 to 250 m² resolution, whereas in Hanover it decreases significantly from 1000 to 500 m² and then increases again at 250 m² resolution (Figure 3: 3b).

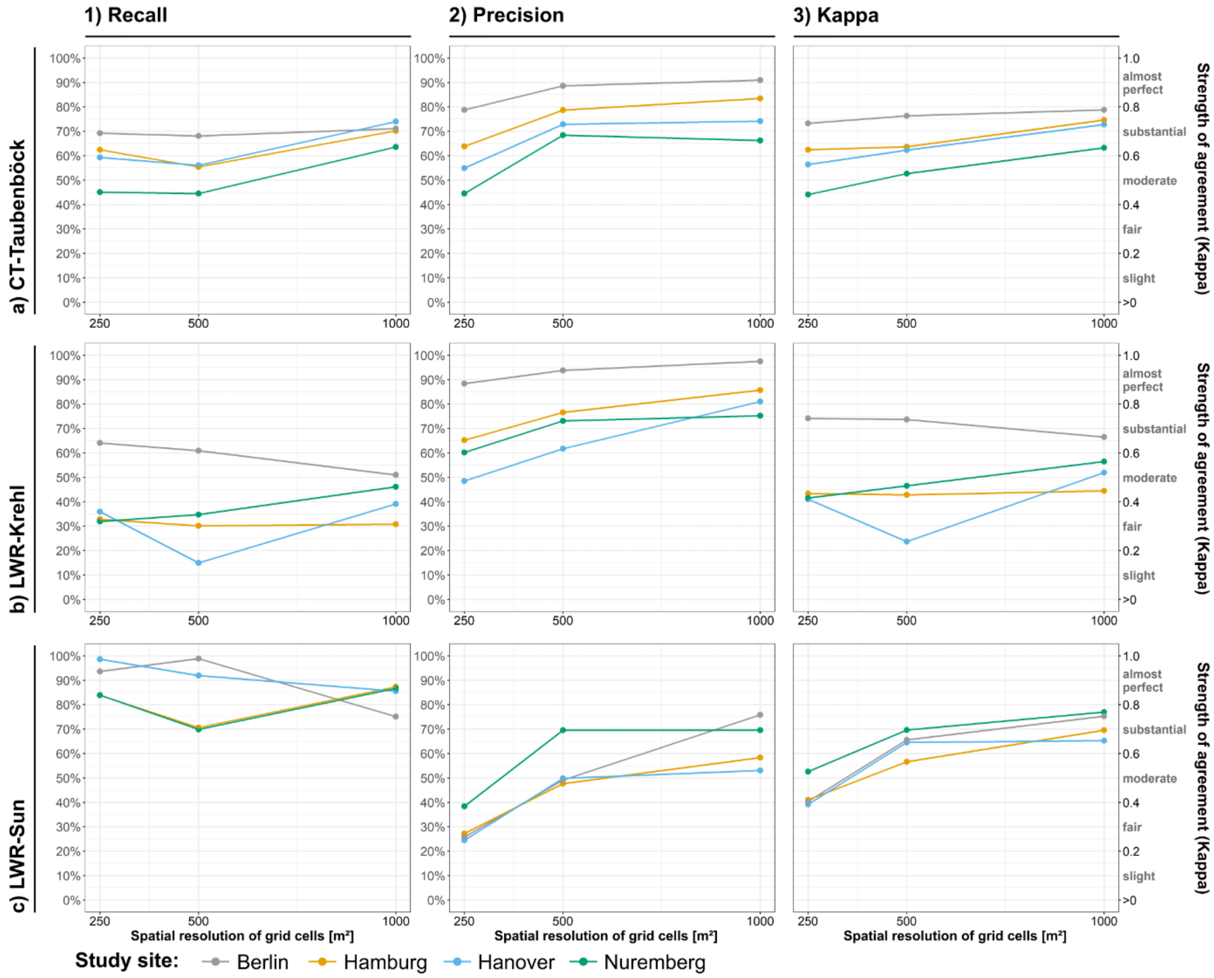

Figure 3: Overview of the results of the spatial agreement between TDX and LoD-1 hUMC grid cells per applied centre identification algorithm (a, b & c). The colours are indicative for the considered study sites.

Next, we present the results of the comparison between the centres identified based on TDX and LoD-1 UMC (*centre-based-agreement*). First, we note that the number (Table 2) and location of the detected TDX and LoD-1 centres varies between the applied centre identification algorithms (see maps Appendix: A/B/C). Most centres are detected with the CT-Taubenböck approach, regardless of the data source and study site. In addition to the core cities, this method identifies a large number of smaller centres in the hinterlands of our study sites. These include other cities/settlements (e.g. Potsdam in the Berlin study site or Lübeck in Hamburg) but also small-scale agglomerations of businesses such as the Technology Park Hennigsdorf close to Berlin. With the LWR-Sun and the LWR-Krehl approaches, we detect significantly fewer centres: only the core cities and few scattered cities/settlements in the hinterlands. Moreover, the area of the identified core cities is smaller compared to those detected with the CT-Taubenböck.

From an urban geographic perspective, all study regions tend to be monocentric (Figure 4), regardless of which polycentricity measure or centre identification algorithm is applied. Berlin, however, is more monocentric than the other cities when looking at the Rank-size/Primacy index (Figure 4: 1/3), while no major differences between the study sites are apparent with the Green index (Figure 4: 2). Nevertheless, the more centre-ranks are considered the less pronounced is the monocentricity of the study sites, in some cases shifting from highly monocentric to predominantly monocentric patterns.

Regarding the agreement between the two data sources, we observe discrepancies in the magnitude of the polycentricity measures obtained from the TDX and LoD-1 centres, respectively. Nevertheless, based on the two data sets, similar monocentricity patterns between the study sites are identified (Figure 4), suggesting a reasonable agreement between TDX- and LoD-1 centres.

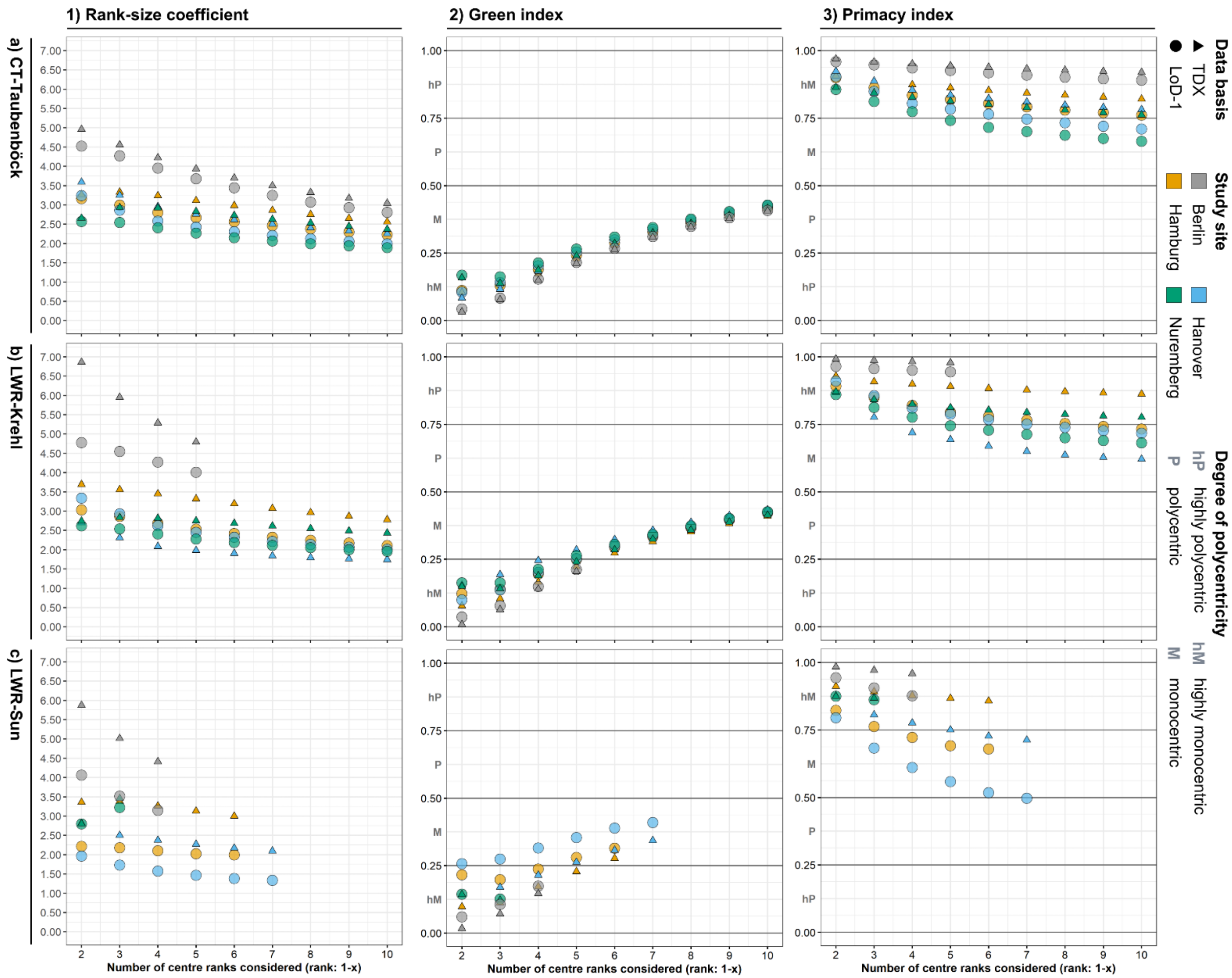

Figure 4: Overview of the results of the applied polycentricity measures (1,2 & 3) per centre identification algorithm (a, b & c) for the different data sources (TDX vs. LoD, circle vs. triangle). The colours are indicative for the considered study sites.

Table 2: Overview of the number of identified centres within the study sites (travel time isochrones) (1-4) per centre identification algorithm (a-c).

		Number of identified centres		
	Algorithm:	**a) CT-Taubenböck**	**b) LWR-Krehl**	**c) LWR-Sun**
Study site:	**1) Berlin**	57/41	9/5	7/4
	2) Hamburg	93/75	43/13	6/10
	3) Hanover	39/37	22/11	7/7
	4) Nuremberg	52/56	22/10	3/3

* LoD-1 centres/TDX centres

3.2) Systematic exploration of factors influencing the agreement between TDX and LoD-1 hUMC cells/centres

First, we focus on our findings of *potential effects stemming from the functionality of the centre identification algorithms* (Figure 5). Of the applied LWR approaches, the LWR-Krehl uses the measured UMC distributions as input while the LWR-Sun relies on the natural logarithm of the same input. Comparing the measured UMC distributions of TDX and LoD-1 (Figure 5: b top), we observe that TDX UMC underestimate LoD-1 UMC. This is particularly pronounced in the fringes of the core city (here Berlin) and in the hinterland. Compared to the respective smoothed UMC distributions, positive residuals are less significant when applying the LWR-Krehl based on TDX UMC instead LoD-1 UMC. We find a large number of FN hUMC cells in these problematic areas (Figure 5: b bottom).

Looking at the natural logarithm of the UMC distributions (Figure 5: c top), we also observe that TDX UMC underestimate the LoD-1 UMC. However, the TDX UMC distribution in the hinterland and the urban fringes is significantly heightened compared to the respective smoothed UMC distribution. Consequently, in these areas, we detect some distinctive hUMC with the LWR-Sun that were missed by the LWR-Krehl when using the TDX data (e.g. Brandenburg a.d. Havel: Figure 5: c/b bottom). Interestingly, we also find that the logarithmized TDX UMC distributions surpass the smoothed UMC distributions in areas where no positive residuals are identified based on LoD-1 data. We therefore detect a certain number of FP hUMC cells with the LWR-Sun (e.g. urban fringe area: Figure 5: c bottom).

The CT-Taubenböck approach uses the measured TDX and LoD-1 UMC distributions as input. In the ring-based example, we also see that TDX UMC underestimate LoD-1 UMC (Figure 5: a top). However, we find larger peaks to be quite pronounced and surpassing the relative threshold of 1.3 standard deviations in both data sets (e.g. Brandenburg a.d. Havel: Figure 5: a bottom).

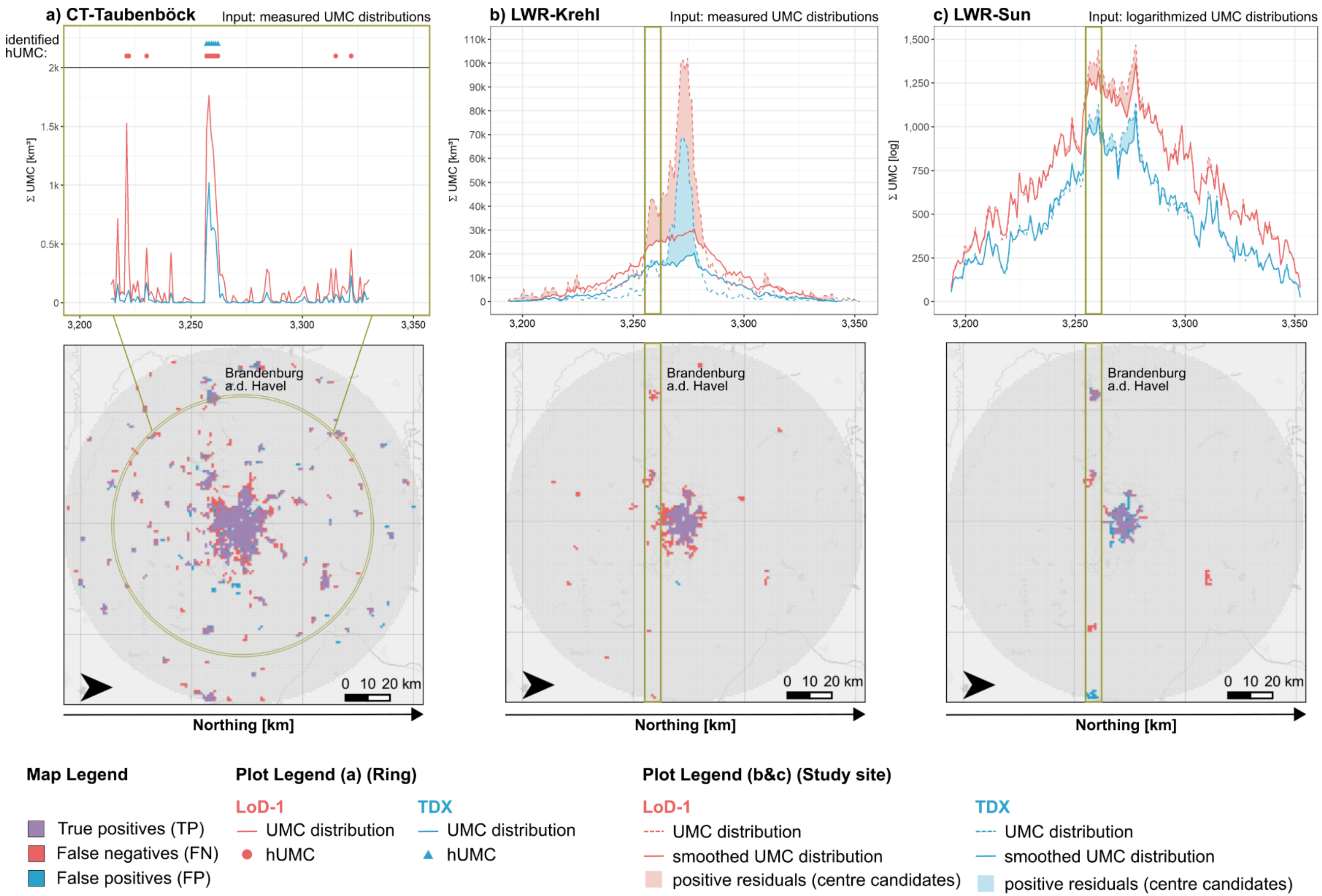

Figure 5: Comparison of the functionality of the applied algorithms for centre identification (a-c) per input data source (TDX and LoD-1) with the agreement between TDX and LoD-1 hUMC cells/centres for the Berlin study site. The top row shows the UMC distributions (TDX and LoD-1) characteristic for the applied algorithms from the northern to the southern boundary of the study site. Next to them, locations with detected TDX and/or LoD-1 hUMC (a) or centre candidates (b,c) cells are highlighted. In the bottom row, validation maps with the location of TP, FP, and FN hUMC cells per algorithm are presented.

Next, we present our results on *effects of the built-up morphology* (Figure 6). Among all considered algorithms and study sites, we observe the agreement between LoD-1 and TDX hUMC cells (TP) to decrease from the classes with highest to those with the lowest density. The built-up height, seems to only have a slight effect on the agreement. We also notice a decrease of TP cells from high to low, but to a much lower extent.

Depending on the algorithm, we additionally find specific types of disagreement in certain morphological classes. In the LWR-Krehl and LWR-Sun approaches, it is the low- and medium-density classes where we observe distinct discrepancies (Figure 6: b/c). In the case of LWR-Krehl, these are mainly caused by FN hUMC cells, while in the context of LWR-Sun, they are primarily induced by FP hUMC cells. Regarding the CT-Taubenböck procedure, the disagreement between TDX and LoD-1 hUMC is mainly restricted to the low-density class. Here, we find a mixture of TP, FP and FN hUMC cells without a clear pattern (Figure 6: a).

Finally, we focus on possible *effects of terrain characteristics*. Independent of the algorithm and the study site, we find that FP hUMC cells are generally characterised by higher relief energy (here standard deviation of slope values) than TP or FN hUMC cells (Figure 7). Among our study sites, we further observe that the variation of slope values is lowest in Berlin and highest in Nuremberg (gradient from low to high: Berlin, Hamburg, Hanover & Nuremberg (Appendix: D)). In line with this, we observe more pronounced relief energy values in FP hUMC cells in Hanover/Nuremberg than in Berlin/Hamburg (Figure 7: 3/4 vs. 1/2).

Regarding the LWR-Krehl and the CT-Taubenböck approaches, we detect the lowest proportion of FP hUMC cells in Berlin and the highest in Nuremberg (Figure 7: a/b top). This finding suggests a relationship between the identified terrain gradient among the study sites and the FP hUMC rate. No such pattern becomes evident with regard to the LWR-Sun. Here, the proportion of FP hUMC cells is highest in Hamburg and Hanover (Figure 7: 1/4c top) and comparatively lower in Berlin and Nuremberg (Figure 7: 2/3c top).

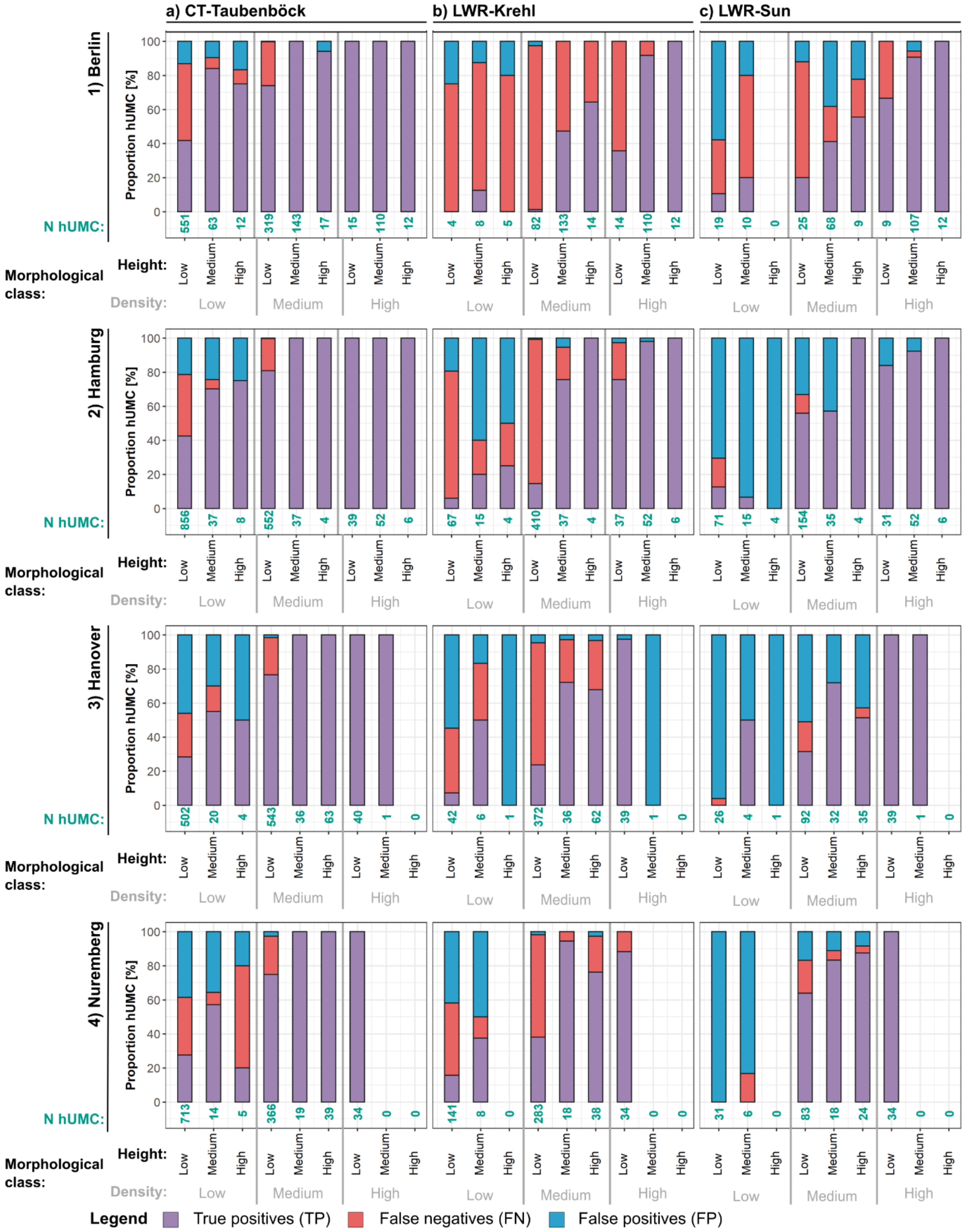

Figure 6: Distribution of TP, FP and FN hUMC cells among nine morphological classes representing combinations of low, medium, and high built-up densities (<10, 10-20, >20%) and heights (<15, 15-25, >25m). The plots are presented per study site (1-4) and applied centre identification algorithm (a-c). Additionally, the number of identified hUMC cells (total of all TP, FP and FN per morphological class) is displayed at the bottom of each plot.

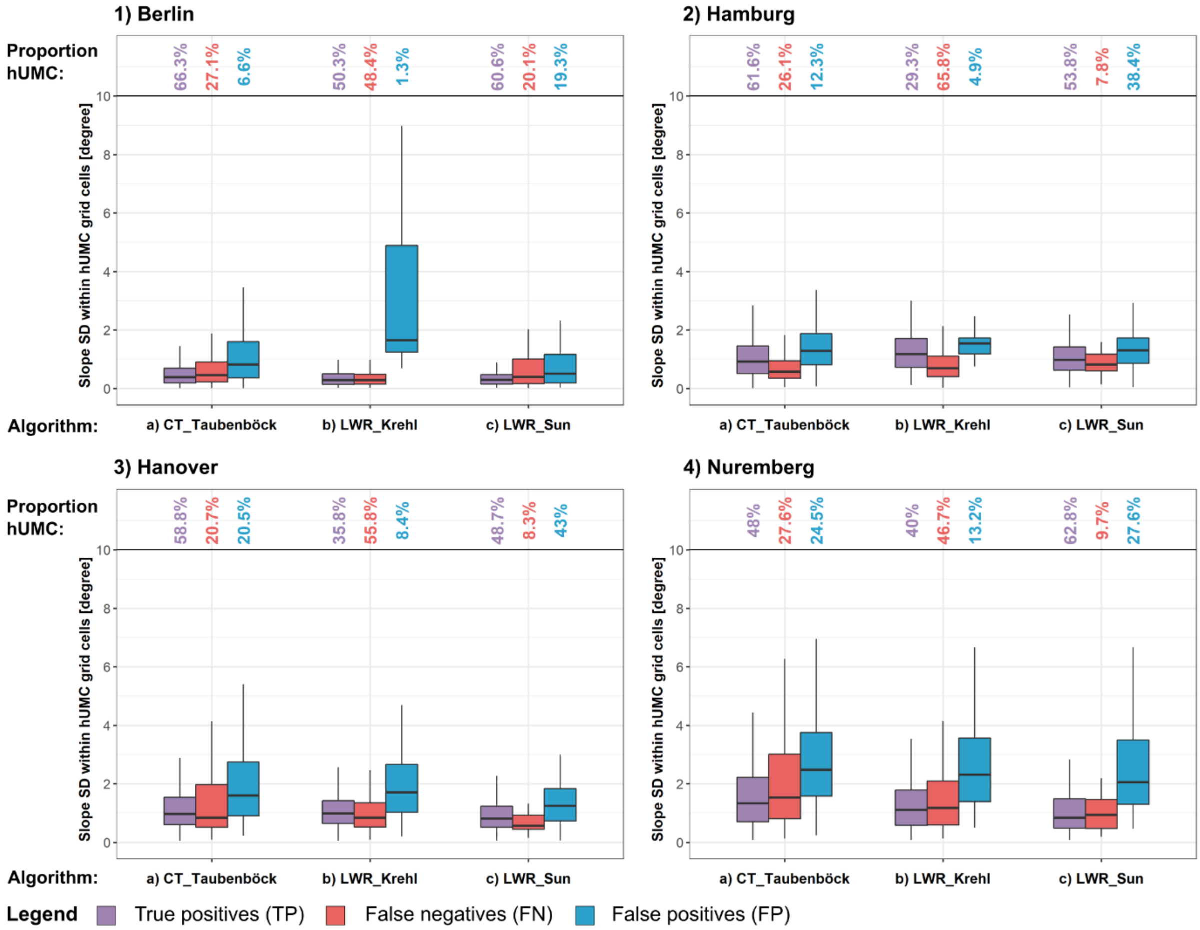

Figure 7: Overview of the distribution of relief energy (here considered as the standard deviation of the slope) among the TP, FP and FN hUMC cells. The plots are presented per study site (1-4) and applied centre identification algorithm (a-c). Additionally, the proportion of TP, FP and FN hUMC cells is displayed at the top of each plot.

4) Discussion and conclusion

Our study aimed at testing whether globally available and consistent TDX built-up volume data permit to detect and analyse intra-urban centre structures in comparable quality than achievable with LoD-1 building models. We find that hUMC cells identified based on LoD-1 and TDX data, exhibit partially moderate, but mostly substantial spatial similarities when superimposed. Accordingly, polycentricity measures computed based on TDX and LoD-1 centres (associations of neighbouring hUMC cells) point towards similar patterns of morphological monocentricity in our study sites. Our results therefore suggest that TDX built-up volumes reflect the distribution of urban built-up structures in sufficient detail so that local-spatial densifications – here equated with centres – can appropriately be detected and analysed.

Geiß et al. (2019) identified an ideal decline of TDX and LoD-1 UMC from urban downtowns to their hinterland. However, LoD-1 heights were found to be generally underestimated by TDX data while LoD-1 built-up densities were overestimated in dense and underestimated in less dense urban areas. In locations with high building densities (e.g. core cities), the underestimation of heights is likely compensated by the overestimation of densities. Accordingly, we find that the core city centres detected based on TDX and LoD-1 UMC, show a high spatial agreement independent of the applied centre identification algorithm and study site. In contrast, areas with less dense building structures – e.g. the urban fringes and the hinterland – are partially smoothed out in the TDX UMC due to the underestimation of heights and densities (Geiß et al. 2019). Consistent with this, we observe that discrepancies between TDX and LoD-1 centres occur primarily in these problematic areas, and are most strongly related to low built-up densities.

As assumed, we find that the applied centre identification algorithms are affected differently by the characteristic underestimations of TDX UMC. With the LWR-Krehl approach, we observe a large portion of FN hUMC cells and accordingly a higher mismatch between the number of TDX and LoD-1 centres (Table 2). This mismatch can result from smaller peaks that are levelled out in the measured TDX UMC (Geiß et al. 2019). Hence, the latter are often not identifiable as significant positive residuals with the LWR-Krehl. Additionally, the iterative removal of hUMC candidates in the algorithm's second step (see section 2.3.4), can react very sensitively to the level of heterogeneity of the input data. Since TDX UMC distributions are smoother relative to LoD-1 UMC distributions, a smaller number of hUMC candidates have a significant influence on the overall UMC distribution. Consequently, fewer hUMC cells are detected based on the TDX data. This inherent property of the algorithm can in extreme cases, such as seen in Hanover (500 m² resolution; Figure 3: 1b), result in only a very small fraction of the LoD-1 hUMC being identified with the TDX hUMC (Recall ~ 20 %).

The LWR-Sun and CT-Taubenböck in contrast, seem to be less impacted by the underestimations of TDX UMC. Using these methods, we still correctly detect more prominent hUMC cells/centres in the problematic areas based on the TDX data. The share of FN hUMC cells is therefore much lower compared to the LWR-Krehl, which is reflected in higher Recall rates of the two approaches.

In terms of the LWR-Sun, two factors likely improve the hUMC cell/centre detection capabilities: First, we find that cells with moderate UMC tend to be more pronounced and therefore identifiable as hUMC, when taking the natural logarithm of the TDX UMC as input. At the same time, however, cells with lower TDX UMC are occasionally emphasized by it, leading to lower Precision values compared to the other approaches. Second, a mismatch between LoD-1 and TDX is less likely in the problematic areas. Here, smaller centres are frequently excluded from both datasets because they do not exceed the significance threshold in the second step of the LWR-Sun. The CT-Taubenböck is generally less restrictive than the LWR methods. UMC cells within a ring must stand out positively to be detected as hUMC cells, but must not be as pronounced as in the LWR approaches. Accordingly, we observe that distinctive centres/hUMC cells in the urban fringes and the hinterland are still correctly identifiable with the measured TDX data.

We find that uneven terrain causes a FP detection of hUMC cells based on TDX data. This aligns with a finding from Geiß et al. (2015), who underline that built-up heights are often overestimated by TDX in areas with steep terrain. The latter can be caused by an insufficient coverage of uneven terrain with “ground pixels” – the basis for DTM interpolation in Geiß et al. (2019) – and/or by mislabeled "ground pixels". Addressing this issue, Geiß et al. (2020) introduced a modified approach that uses a combination of Sentinel-2 imagery and geospatial vector data from the Open Street Map project in addition to the morphological filtering for the “ground pixel” detection. The method was tested in Santiago de Chile, Chile, an urban region with heterogeneous terrain, and could significantly improve terrain height estimates but was not yet fully developed when we implemented this research. However, we recommend to test, if it can improve the centre identification in regions with complex terrain in future works where the required additional data, i.e., Sentinel-2 and OSM data, can be compiled for the area under study.

Despite the challenges, we find intra-urban centre structures to be detected sufficiently based on TDX UMC data. The polycentricity measures calculated based on both, TDX and LoD-1 centres, indicate similar patterns: In general, all our study sites display rather monocentric patterns. This reflects the view that German urban regions are far less polycentric than for instance their counterparts in the US, and that (sub-)centres in Germany rather complement than replace the functions of the core city (Krehl and

Siedentop 2018, Münter and Volgmann 2020, Heider et al. 2022). Berlin is, compared to the other study sites, by far the most monocentric region when considering the Rank-size-/Primacy index. This can be explained by the large size of the core city itself and its relatively isolated location with only a few significantly smaller cities (e.g. Potsdam) in the immediate hinterland. Whether a region is polycentric/monocentric is often determined considering only few of the largest-ranked centres (here ten) (Meijers 2008). Smaller centres, for which we found lower spatial agreement between TDX and LoD-1 (e.g. LWR-Krehl), are thus not included in the calculation of the polycentricity measures. Accordingly, we witness similar patterns of monocentricity among all centre identification approaches and data sources.

While our findings highlight the potential of TDX UMC for investigations of intra-urban polycentricity, some challenges remain: First, the LoD-1 cadastral building model, which builds the reference of our analysis, is not an unbiased dataset. Due to the federal administrative structure in Germany, different states use different reference values – e.g. median or mean – to calculate building heights. Additionally, laser scanning data are not collected with the same sensors everywhere or the building heights are partly derived with other means (e.g. photogrammetry) (ADV 2012). Although we tried to homogenize the LoD-1 in advance, some inconsistencies remain. Accordingly, we observe lower Recall/Precision values in Hamburg/Hanover – both study sites span across Lower Saxony - when applying the LWR approaches. These discrepancies between TDX and LoD-1 cannot be attributed to the characteristic underestimations of TDX UMC and are thus, likely resulting from inconsistencies of the LoD-1. Most of the mismatches between TDX and LoD-1 centres, however, can yet be related to the characteristic flaws of the TDX data. Hence, we are confident that the LoD-1 inconsistencies had only a minor impact on our results.

Second, although we aim to highlight the capabilities of TDX UMC for large-scale application, our study only considers German study sites. This choice is justified by data availability, as we only had access to LoD-1 data from this country. However, building structures are likely varying across different geographic regions and thus, may affect TDX UMC estimates differently. Besides, within our study sites, high relief energy is mainly occurring in the low-density classes (Appendix: E). In other cities, steep terrain is likely to be found on a larger range of morphological classes. From our findings, we cannot infer if and how these properties can affect the detection and analysis of intra-urban centres. However, we believe that the urban regions considered here are sufficient for a proof-of-concept, i.e., that TDX UMC are suitable for examining intra-urban polycentricity based on built-up volumes. Nevertheless, we suggest to extend our research to urban regions with different geographic context and heterogeneous terrain in future studies.

Overall, our study shows that TDX data – despite their coarser spatial resolution – enables to map local-spatial densifications of built-up volumes in comparable detail to what is achievable with LoD-1 data. Caution should yet be exercised on uneven terrain and sparsely built-up areas, as well as in the choice of centre identification algorithms. We find these factors can affect the validity of the TDX UMC estimates and/or detected centres. Despite the remaining challenges and future research needs, we highlighted the potential of TDX UMC for thematic morphological urban analyses at large scales, such as those addressing intra-urban polycentricity based on built-up volumes. Furthermore, an application of TDX UMC for the detection and analysis of centres at higher spatial resolution is conceivable. Not least, we have shown that a good spatial correspondence between TDX and LoD-1 hUMC cells is still given at 500 m^2 resolution. Yet, polycentricity as a specific form of urban spatial structure, is multi-faceted and should be studied by incorporating information that characterize their different dimensions (Krehl 2015). The combination of TDX UMC with LandScan data (Dobson et al. 2000), for example, provides a unique opportunity to meet this requirement and perform multidimensional analyses of intra-urban polycentricity at large spatial scales in the future. Beyond capturing the physical dimension of urban spatial structure, UMC data are also considered as proxy for employment figures, which are often not easily available on large extents (Heider and Siedentop 2020). Although Krehl (2015) has already demonstrated that a correlative relation between the distribution of UMC and employees exists, we recommend that future studies examine the spatial dimension of this relationship in more detail. Apart from these perspectives of further use, TDX data have an inherent drawback: they are not systematically reproduced over time. Hence, other surrogates for multitemporal analyses must be found.

References

ADV, Arbeitsgemeinschaft der Vermessungsverwaltungen der Länder der Bundesrepublik Deutschland. 2012. Produktstandard für 3D Gebäudemodelle - LoD-1.

Agarwal, A., G. Giuliano, and C. L. Redfearn. 2012. Strangers in our midst: the usefulness of exploring polycentricity. The Annals of Regional Science 48:433–450.

Anas, A., R. Arnott, and K. A. Small. 1998. Urban spatial structure. Journal of economic literature 36:1426–1464.

Bartosiewicz, B., and S. Marcinczak. 2020. Investigating polycentric urban regions: Different measures – Different results. Cities 105:102855.

BKG, Bundesamt für Kartographie und Geodäsie. 2016. Digitales Geländemodell Gitterweite 25 m - DGM25.

BKG, Bundesamt für Kartographie und Geodäsie. 2021. Dokumentation 3D Gebäudemodell Deutschland - LoD-1.

Burger, M. J., B. de Goei, L. van der Laan, and F. J. M. Huisman. 2011. Heterogeneous development of metropolitan spatial structure: Evidence from commuting patterns in English and Welsh city-regions, 1981–2001. Cities 28:160–170.

Burger, M., and E. Meijers. 2012. Form follows function? Linking morphological and functional polycentricity. Urban studies 49:1127–1149.

Champion, A. G. 2001. A changing demographic regime and evolving polycentric urban regions: Consequences for the size, composition and distribution of city populations. Urban Studies 38:657–677.

Congalton, R. G. 1991. A review of assessing the accuracy of classifications of remotely sensed data. Remote Sensing of Environment 37:35–46.

Derudder, B., X. Liu, M. Wang, W. Zhang, K. Wu, and F. Caset. 2021. Measuring polycentric urban development: The importance of accurately determining the “balance” between ‘centers. Cities 111:103009.

Dobson, J. E., E. A. Bright, P. R. Coleman, R. C. Durfee, and B. A. Worley. 2000. LandScan: a global population database for estimating populations at risk. Photogrammetric engineering and remote sensing 66:849–857.

EEA, European Environmental Agency. 2017. European INSPIRE Grid.

Esch, T., H. Taubenböck, A. Roth, W. Heldens, A. Felbier, M. Schmidt, A. A. Mueller, M. Thiel, and S. W. Dech. 2012. TanDEM-X mission-new perspectives for the inventory and monitoring of global settlement patterns. Journal of Applied Remote Sensing 6:061702.

Garreau, J. 1991. Edge city: Life on the new frontier. . Anchor.

Geiß, C., T. Leichtle, M. Wurm, P. A. Pelizari, I. Standfuß, X. X. Zhu, E. So, S. Siedentop, T. Esch, and H. Taubenböck. 2019. Large-Area Characterization of Urban Morphology—Mapping of Built-Up Height and Density Using TanDEM-X and Sentinel-2 Data. IEEE Journal of Selected Topics in Applied Earth Observations and Remote Sensing 12:2912–2927.

Geiß, C., P. A. Pelizari, S. Bauer, A. Schmitt, and H. Taubenbock. 2020. Automatic Training Set Compilation With Multisource Geodata for DTM Generation From the TanDEM-X DSM. IEEE Geoscience and Remote Sensing Letters 17:456–460.

Geiß, C., M. Wurm, M. Breunig, A. Felbier, and H. Taubenböck. 2015. Normalization of TanDEM-X DSM Data in Urban Environments With Morphological Filters. IEEE Transactions on Geoscience and Remote Sensing 53:4348–4362.

Giuliano, G., and K. A. Small. 1991. Subcenters in the Los Angeles region. Regional Science and Urban Economics 21:163–182.

Glaeser, E. L. (Edward L., and M. E. Kahn. 2001. Decentralized Employment and the Transformation of the American City. Brookings-Wharton Papers on Urban Affairs 2001:1–63.

Gordon, P., and H. W. Richardson. 1996. Beyond Polycentricity: The Dispersed Metropolis, Los Angeles, 1970-1990. Journal of the American Planning Association 62:289–295.

Graham, M. R., M. J. Kutzbach, and B. McKenzie. 2014. Design Comparison of LODES and ACS Commuting Data Products. . Center for Economic Studies, U.S. Census Bureau.

Green, N. 2007. Functional Polycentricity: A Formal Definition in Terms of Social Network Analysis. Urban Studies 44:2077–2103.
Hall, P. G., and K. Pain. 2006. The polycentric metropolis: learning from mega-city regions in Europe. . Routledge.
Heider, B., J. Mast, D. Roth, I. Standfuß, S. Siedentop, and H. Taubenböck. 2022. Dynamics of intra-urban employment geographies: A comparative study of U.S. and German metropolitan areas. Journal of Urban Affairs:1–21.
Heider, B., and S. Siedentop. 2020. Employment suburbanization in the 21st century: A comparison of German and US city regions. Cities 104:102802.
Kim, S. 2007. CHANGES IN THE NATURE OF URBAN SPATIAL STRUCTURE IN THE UNITED STATES, 1890-2000ast. Journal of Regional Science 47:273–287.
Kloosterman, R. C., and S. Musterd. 2001. The Polycentric Urban Region: Towards a Research Agenda. Urban Studies 38:623–633.
Krehl, A. 2015. Urban spatial structure: an interaction between employment and built-up volumes. Regional Studies, Regional Science 2:290–308.
Krehl, A. 2016. Urban subcentres in German city regions: Identification, understanding, comparison. Papers in Regional Science 97:S79–S104.
Krehl, A., and S. Siedentop. 2018. Towards a typology of urban centers and subcenters – evidence from German city regions. Urban Geography 40:58–82.
Krehl, A., S. Siedentop, H. Taubenböck, and M. Wurm. 2016. A Comprehensive View on Urban Spatial Structure: Urban Density Patterns of German City Regions. ISPRS International Journal of Geo-Information 5:76.
Landis, J. D. 2006. Growth Management Revisited: Efficacy, Price Effects, and Displacement. Journal of the American Planning Association 72:411–430.
Landis, J. R., and G. G. Koch. 1977. The Measurement of Observer Agreement for Categorical Data. Biometrics 33:159.
Lang, R. E., and J. LeFurgy. 2003. Edgeless cities: examining the noncentered metropolis. Housing Policy Debate 14:427–460.
Li, Y., and B. Derudder. 2020. Dynamics in the polycentric development of Chinese cities, 2001-2016. Urban Geography 43:272–292.
Liu, X., B. Derudder, and M. Wang. 2017. Polycentric urban development in China: A multi-scale analysis. Environment and Planning B: Urban Analytics and City Science 45:953–972.
Liu, X., and M. Wang. 2016. How polycentric is urban China and why? A case study of 318 cities. Landscape and Urban Planning 151:10–20.
McMillen, D. P. 2001. Nonparametric Employment Subcenter Identification. Journal of Urban Economics 50:448–473.
Meijers, E. 2008. Measuring Polycentricity and its Promises 16:1313–1323.
Münter, A., and K. Volgmann. 2020. Polycentric regions: Proposals for a new typology and terminology. Urban Studies 58:677–695.
Parr, J. 2004. The Polycentric Urban Region: A Closer Inspection. Regional Studies 38:231–240.
Siedentop, S., S. Fina, and A. Krehl. 2016a. Greenbelts in Germany’s regional plans—An effective growth management policy? Landscape and Urban Planning 145:71–82.
Siedentop, S., A. Krehl, D. Guth, and C. Holz-Rau. 2016b. Morphologische Polyzentralität der Beschäftigung in deutschen Metropolregionen – Aktuelle Befunde und Veränderungen seit 1970. Pages 45–75 *in* R. Danielzyk, A. Münter, and T. Wiechmann, editors. Verlag Dorothea Rohn.
Sun, T. 2019. A longitudinal study of changes in intra-metropolitan employment concentration in Beijing: Decentralisation, reconcentration and polycentrification. Urban Studies 57:748–765.
Taubenböck, H., I. Standfuß, M. Wurm, A. Krehl, and S. Siedentop. 2017. Measuring morphological polycentricity - A comparative analysis of urban mass concentrations using remote sensing data. Computers, Environment and Urban Systems 64:42–56.
Taubenböck, H., M. Wiesner, A. Felbier, M. Marconcini, T. Esch, and S. Dech. 2014. New dimensions of urban landscapes: The spatio-temporal evolution from a polynuclei area to a mega-region based on remote sensing data. Applied Geography 47:137–153.

Wurm, M., P. dAngelo, P. Reinartz, and H. Taubenbock. 2014. Investigating the Applicability of Cartosat-1 DEMs and Topographic Maps to Localize Large-Area Urban Mass Concentrations. IEEE Journal of Selected Topics in Applied Earth Observations and Remote Sensing 7:4138–4152.

Zhang, W., and B. Derudder. 2019. How sensitive are measures of polycentricity to the choice of “centres”? A methodological and empirical exploration. Urban Studies 56:3339–3357.